Catalysis Today 418 (2023) 114128

Contents lists available at ScienceDirect

Catalysis Today

journal homepage: www.elsevier.com/locate/cattod

On the role of multifunctional ionic liquids for the oxidative carboxylation of olefins with carbon dioxide

Natália Podrojková [a,1], Andrej Oriňak [a,2], Eduardo Garcia-Verdugo [b,3], Victor Sans [c,4,*], Marcileia Zanatta [c,5,*]

[a] Department of Physical Chemistry, Faculty of Science, Pavol Jozef Šafárik University in Košice, Moyzesova 11, Košice 04001, Slovakia
[b] Departamento de Química Inorgánica y Orgánica, Grupo de Química Sostenible y Supramolecular Universidad Jaume I, E-12071 Castellón, Spain
[c] Institute of Advanced Materials (INAM), Univesitat Jaume I, Avda Sos Baynat s/n, 12071 Castellón, Spain

ARTICLE INFO

Keywords:
Ionic Liquids
Catalysis
DFT
CO_2 cycloaddition
Olefin oxidation

ABSTRACT

Ionic liquids (ILs) are catalysts with profound effects on the activity and selectivity for the transformation of CO_2. In particular, highly functionalisable and immobilisable imidazolium based ILs (ImILs) activate CO_2 molecules and have demonstrated activity towards CO_2 cycloaddition reactions. The addition of hydroxyl groups has also been reported to enhance the cycloaddition reaction. An ideal system would combine both functionalities for superior performance. In addition, integrating the cycloaddition with the epoxidation of olefins employing multifunctional catalysts in one-pot would improve process efficiency, reduce waste and costs. However, the interaction between the cation-anion and the hydroxyl groups needs to be elucidated to realize these advantages. Herein, the viability of using ILs as bifunctional catalyst for one-pot reaction is evaluated by combining theoretical and experimental studies. Density functional theory (DFT) simulations of both reactions using halogenated and hydroxyl functionalized ImLs are presented. The position of the hydroxyl group close to the imidazolium unit primarily influences the opening of the epoxide and its activation for the cycloaddition reaction, thus facilitating the catalysis. In addition, experimentally the selectivity increases considerable with the catalyst immobilization. For the epoxidation reaction the DFT calculations and experimental results demonstrated favoring hydrolysis reaction.

1. Introduction

Carbon dioxide is the most abundant greenhouse gas and has recently attracted the world's attention. The anthropogenic activities result in rapid carbon cycles producing approximately 30 billion tons of CO_2 per year [1]. The increase in the atmospheric concentration of CO_2 has been associated with an increase in global temperatures [1–3]. In order to achieve the grand challenge of a net-zero emission societies, it is imperative to develop carbon neutral and carbon negative chemical processes. From this point of view, it is highly interesting the conversion of CO_2 from waste gas into feedstock for the synthesis of various chemicals, since CO_2 is a cheap, non-toxic, and most abundant renewable source of C_1 [4–6]. Currently, CO_2 is used in the industry to produce methanol, carboxylic acids, urea, and cyclic carbonates, mainly by thermochemical processes [7,8].

One of the promising methods of CO_2 conversion into useful chemicals is the insertion of CO_2 into the structure of epoxides to form cyclic carbonates that can be used as electrolytes for batteries [9,10], aprotic polar solvents [11–13], valuable starting materials for polymerization reactions [14–16] and intermediates in organic synthesis [5,17,18]. Another benefit of this transformation is to replace classic industrial processes using phosgene ($COCl_2$) with a much more ecological precursor of C_1 building unit [2,4,19]. The cycloaddition of CO_2 into the structure of epoxides has an optimal atom economy [17,20–22].

* Corresponding authors.
E-mail addresses: sans@uji.es (V. Sans), zanatta@uji.es (M. Zanatta).
[1] 0000-0002-4187-3583
[2] 0000-0001-6624-9907
[3] 0000-0001-6867-6240
[4] 0000-0001-7045-5244
[5] 0000-0002-3080-3627

https://doi.org/10.1016/j.cattod.2023.114128
Received 19 November 2022; Received in revised form 25 February 2023; Accepted 18 March 2023
Available online 23 March 2023

Homogeneous catalysts are highly efficient, but their application is problematic due to the cumbersome product separation, and difficulty to recover the catalyst, typically composed of metals and/or ligands [21,23]. In contrast, heterogeneous catalysts can be easily separated from the products and reutilized in subsequent reaction cycles. However, their catalytic efficiency is still relatively low compared to homogeneous counterparts [24] and catalytic processes usually require solvents, additives and demanding conditions such as high temperature, high pressure, or high purity of the supplied CO_2 [21,24].

Ionic liquids (ILs) are promising catalysts for cycloaddition of CO_2 to epoxides to form cyclic carbonates [25–27]. ILs are organic salts with interesting properties such as low vapor pressure, good thermal stability, polarity and hydrophilicity, unique solvation properties, low volatility, high ionic conductivity, wide electrochemical window, adjustable structure and as well catalytic activity and selectivity [19,26]. ILs can also be encapsulated or supported in solid materials to form supported ionic liquid (SILs), which overcomes limitations such as high cost and difficulty in separation and transportation [19]. Although the SILs serve as heterogeneous catalysts, generally their catalytically active components are given in liquid form on the inner surface of the pores of the solid support. Due to these unique properties, SILs improve mass transfer, promote reusability, and overall provide the same advantages as homogeneous catalysts [19,28,29].

Regarding the use of ILs or SILs as catalyst for the cycloaddition of CO_2 to epoxides, usually the reactions are performed with temperatures between 100 and 150 °C, pressures of 5–100 bar and with a reaction time of 2–70 h, presenting moderate to good (50–100 %) selectivity and conversion [19,27]. Imidazolium-based ILs (ImILs) are the most common IL-based catalysts employed, since they can be easily functionalized and can activate CO_2 molecules [30,31]. Saptal and Bhanage presented the synergic effect of the OH group of choline and NH_2 group of amino acid on epoxide and CO_2 activation during CO_2 cycloaddition to epoxides under solvent-free conditions using bifunctional IL derived from choline and histidine [Ch][His] [32]. We have recently reported a methodology to functionalise 3D printed polymers containing hydroxyl and imidazolium catalytic moieties and demonstrated their efficiency for CO_2 cycloaddition reaction [33]. Despite the high activity observed, a profound understanding of the exact mechanism is necessary to develop the next generation of catalysts for this challenging transformation.

Additionally, the combination of CO_2 cycloaddition with epoxidation of olefins could simplify the industrial processes mainly by avoiding the separation and purification of epoxides. This is highly desirable from an economic and environmental point of view. [34–38]. For example, Sun et al. employed the direct synthesis of styrene carbonate (SC) from styrene and CO_2 using tert-Butyl hydroperoxide (TBHP) as oxidant in the presence of tetrabutylammonium bromide (TBAB) resulting in 38 % SC yield which is not satisfactory for practical applications [34]. Jasiak et al. carried out one-pot synthesis in the presence of Au/CNT-[bmim]Br-$ZnBr_2$ at 100–120 °C under 1.2 MPa of CO_2 for 6 h with overall yield of 60 % [35]. Oxidative carboxylation of styrene was also investigated by Liu et al. applying imidazolium hydrogen carbonate ILs as catalyst with 91 % conversion of styrene and 82 % selectivity towards SC at 65 °C for 30 h [36]. Moreover, ILs were supported on dendrimeric silica fibers nanoparticles by Cui and Shamsa which led to 99 % yield of SC under 10 bar of CO_2, 60 °C for 1 h [37]. Recently, Long et al. demonstrated improved dual function of amino-functionalized ILs@SBA-15 via mechanochemical grafting under 80 °C, 10 bar of CO_2 with 28 h reaction time, catalysing the oxidation of styrene with 98 % conversion and 67 % yield of styrene oxide and promoting cycloaddition reaction towards styrene carbonate with 100 % conversion and 99 % yield [38]. In general, even though there are still shortcomings such as the high amount of catalyst used, demanding reaction conditions, and problematic product separation, these studies point to the great potential of ionic liquids and room for improvement of their catalytic properties.

The deep understanding of the reaction mechanism of the coupled reaction system and the role of the catalyst' structure is of paramount importance to design an adequate and efficient catalytic process. Furthermore, the possibility to immobilise the catalysts is crucial to facilitate the separation, reutilisation of the catalyst and to develop continuous-flow processes. For these reasons, and based on our recently reported polymeric ionic liquids [33], we have studied in depth the influence of cation, anion and hydroxyl groups closely located to the imidazole moieties in a multifunctional IL catalyst. The mechanism of CO_2 cycloaddition reaction using DFT calculations was evaluated. In addition, the performance of the catalyst for epoxidation of alkenes followed by CO_2 cycloaddition (*one-pot)* was also simulated, in order to evaluate a further use as multifunctional system. Finally, theoretical simulations were compared with experimental results and the role of ILs and hydroxyl in each reaction group has been determined.

2. Material and methods

2.1. Methodology of computational calculations

Computational calculations were carried out in the framework of standard density functional theory (DFT) at 0 K using general gradient approximation (GGA) of Perdew-Burke-Ernzerhof (PBE) functional [39,40]. All calculations were performed by Quantum ESPRESSO distribution using Plane-Wave (PW) basis set and pseudopotential (PP) method with projector augmented wave method (PAW) PPs under Plane-Wave Self-Consistent Field (PWscf) code [41–43]. A kinetic energy of 50 Ry for wave-functions and charge density cutoff of 330 Ry were applied. Gaussian smearing value of 0.002 Ry was used for SCF convergence improvement with convergence threshold of 10^{-6} Ry. The structures were simulated in a cell with a size of 30 Å in each direction.

The presence of transition states connecting reactants and products for styrene epoxidation and CO_2 cycloaddition was confirmed performing Climbing image-nudge elastic band (CI-NEB) method [44,45] using Plane-Wave Nudge elastic band (PWneb) code. From the collected CI-NEB images the TS is determined based on the values of the resulting optimized energy of each CI-NEB image (Figs. S4 and S5). To determine and calculate the reaction energy equation below was applied (Eq. 1):

$$E_i = E_S - (E_{CO2} + E_{IL} + E_M) \quad (1)$$

where E_i is the energy of the interaction in eV, E_S is the total energy of the optimised system in eV, E_{CO2} is the energy of the optimised isolated molecule CO_2, E_{IL} is the energy of the optimised isolated molecule IL and E_M is the energy of the optimised isolated molecule of styrene oxide reactant or SC product.

The systems were visualized using the VESTA and the UCSF ChimeraX package. Graphs with reaction coordinates were prepared using MechaSVG [46]. The molecules were not fixed to find the most ideal atom positions, bond lengths, and shape of the structures with the lowest system energy.

2.2. Experimental methodology

All reagents and solvents used were commercially available and used as received. The complete list of reagents, ILs synthesis and characterization can be found in the electronic supporting information (ESI).

2.2.1. Cycloaddition reaction

Catalysts (0.5 mmol, 10 mol %) were charged into a Parr reactor with a magnetic stirrer bar. Styrene oxide (5 mmol, 0.572 mL) was added, and the reactor was sealed and flushed 3 times at room temperature with N_2, vacuum and then CO_2 to remove the air from the vessel. The pressure was adjusted to 5 bar. The reaction was stirred at 100–150 °C for 4 h. After this reaction, the reactor was cooled to room temperature and the pressure was released. The conversion and selectivity to styrene carbonate was calculated by ^{1}H NMR spectroscopy.

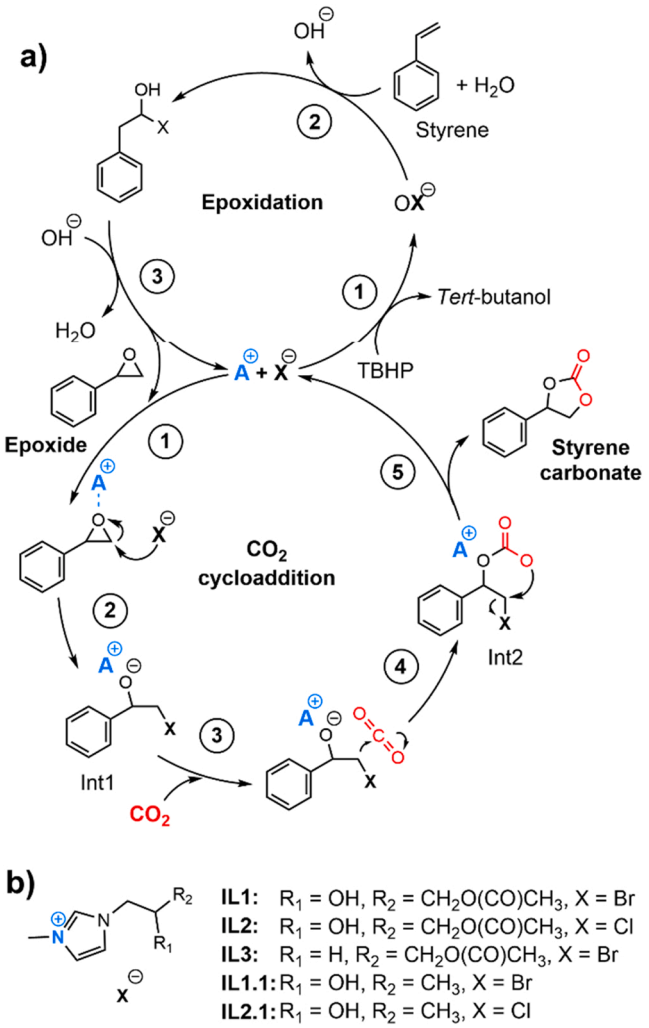

Fig. 1. a) General mechanism of cyclic oxidation for styrene oxide formation and subsequent CO_2 cycloaddition for styrene carbonate formation in the presence of IL according to the literature [50]. b) Structure of ImILs used in this study.

2.2.2. Oxidation reaction with sequential cycloaddition reaction: step 1

Catalysts (0.5 mmol, 10 mol %) were charged into a Parr reactor with a magnetic stirrer bar. Styrene (5 mmol, 0.572 mL) and TBHP (7.5 mmol, 1.04 mL) were added, and the reactor was sealed and flushed 3 times at room temperature with N_2 and vacuum. The reaction was stirred at 100 °C for 2 h. *Step 2:* After this reaction, the reactor was pressurized with 5 bar of CO_2. The reaction was stirred at 100 °C for 4 h. The conversion and selectivity to styrene carbonate was calculated by ^{1}H NMR spectroscopy.

2.2.3. One-pot oxidative carboxylation of styrene with CO_2

Catalysts (0.5 mmol, 10 mol %) were charged into a Parr reactor with a magnetic stirrer bar. Styrene (5 mmol, 0.572 mL) and TBHP (7.5 mmol, 1.04 mL) were added, and the reactor was sealed and flushed 3 times at room temperature with N_2, vacuum and then CO_2 to remove the air from the vessel. The pressure was adjusted to 5 bar. The reaction was stirred at 100 °C for 6 h. After this reaction, the reactor was cooled to room temperature and the pressure was released. The conversion and selectivity to styrene carbonate was calculated by ^{1}H NMR spectroscopy.

3. Results and discussion

3.1. DFT calculations: CO_2 cycloaddition reaction to epoxide

Several studies have reported the general mechanism of CO_2 cycloaddition to epoxides [47–49]. Sun et al. also proposed the mechanism for direct synthesis of styrene carbonate from styrene and CO_2 with TBHP in the presence of TBAB [50]. Fig. 1a represents a possible one-pot mechanism of cyclic oxidation of styrene and sequential CO_2 cycloaddition. According to this mechanism, the formation of styrene oxide in the presence of IL involves 3 steps: catalytic oxidation of X^- with TBHP which leads to formation of a hypohalite OX^- (step 1); halogenation of styrene in the presence of H_2O with formation of halohydrin (step 2) and base-promoted dehydrohalogenation of halohydrin leading to styrene epoxide (step 3). Subsequently, the styrene oxide cycloaddition involves 5 steps and the IL plays multiple roles in it: provides a Lewis acid site to activate the styrene epoxide by interacting with the oxygen atom (step 1) and a basic site to open the ring of the activated styrene oxide through nucleophilic attack, commonly on the more accessible carbon atom of the styrene oxide (step 2). This leads to the formation of a styrene alkoxide intermediate (Int 1). The stability of this ring-opened styrene oxide is being provided by the counter-cation. This is a key factor for the rapid insertion of CO_2 under mild reaction conditions. Int 1 subsequently undergoes CO_2 insertion to form a styrene carbonate intermediate (Int 2, steps 3 and 4). Since CO_2 has a partially positive and partially negative charge on the carbon and oxygen atoms, the activation of CO_2 can be accomplished by either nucleophilic or electrophilic attack. The resulting Int 2 undergoes intra-molecular displacement of the halide anion by a nucleophilic substitution mechanism. Finally, the styrene carbonate is formed, and the catalyst is regenerated (step 5) [41].

Similar steps were considered in this work to simulate both reactions. In first place we focused on the CO_2 cycloaddition reaction. Based on our previous study [33], different IL structures (Fig. 1b, **IL1**, **IL2** and **IL3**) analogous to the immobilised ILs [ImIL containing hydroxyl and ester group from glycidyl methacrylate polymerization] were simulated with DFT calculations and compared to experimental work to reach a better understanding of the functionalization effect on the reaction mechanism.

Firstly, the molecules of the system studied, namely CO_2, styrene oxide, SC and the ImILs (Fig. 1b) were optimised employing DFT calculations. The electrostatic potential surface was mapped at electron density at isovalue of 0.1 a.u. to analyse regions with excess electrons and electron deficiency, see ESI for more details. Employing the optimised molecules and electrostatic potential map analysis of **IL1**, two feasible positions of Br anion near IL2 molecule were determined (Fig. S1 and S2, Table S1). According to the interaction energy of optimised configurations (Fig. S1d and e, Table S1), Br1 atom prefers the position near methyl group of IL1 molecule. Thus, two possible configurations were analysed which led to two different reaction pathways of CO_2 cycloaddition into the styrene oxide structure.

The first initial configuration of the system (Fig. 2a) is based on the Br1 atom located near the CH_3 group of the IL and near the C2 atom of styrene oxide, while the styrene oxide O1 atom interacts with the H1 atom of IL and the C1 atom of the CO_2 molecule is located near the styrene oxide O1 atom (Fig. 2b). The hydroxyl group of the IL responds to the presence of the epoxide by orienting the H1 atom toward the O1 atom of the epoxide and changing the bond length between the H1 and O2 of –OH group against the optimised isolated IL from $d_{(H1\text{-}O2)}$ = 0.975 Å to $d_{(H1\text{-}O2)}$ = 0.981 Å.

Alternatively, Br1 atom could be located near the H1 atom of hydroxyl group (Fig. 2b). The epoxide is oriented by the C2 atom to the Br1 atom and the distance between them is $d_{(Br1\text{-}C2)}$ = 3.005 Å, lesser compared to the first configuration of the system. Compared to the first system configuration the distance is greater than the distance between the O1 atom of epoxide and the atom H1 of hydroxyl group of the first

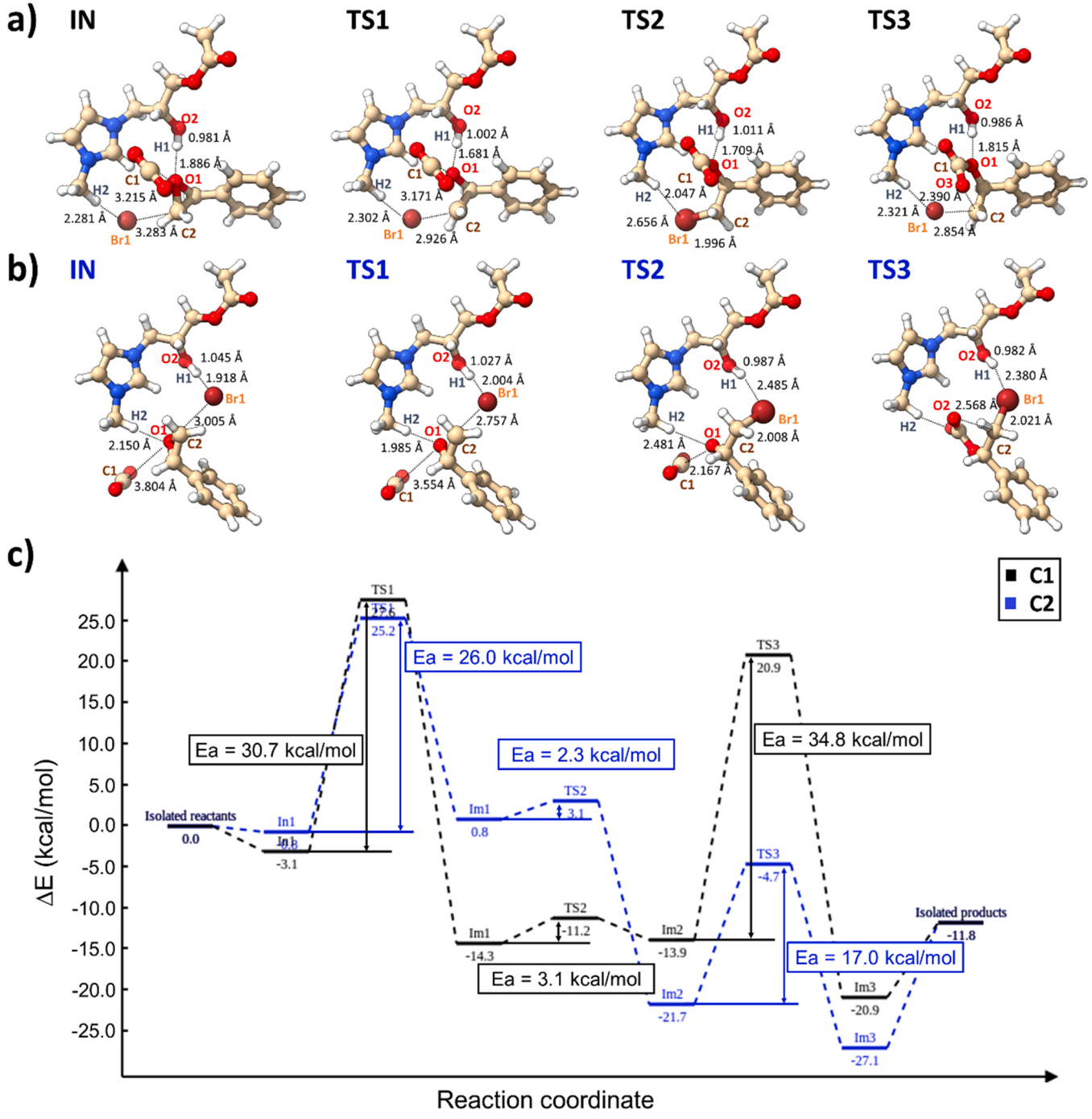

Fig. 2. Optimised IN, TS1, TS2, TS3 using **IL1** for a) C1 and b) C2; c) comparison of potential energy profiles of C1 and C2.

system configuration.

After optimisation, the individual transition states were determined, thus completing the reaction pathways (see ESI for more details, Fig. S3-S8). The reaction coordinate of reaction C1 and C2 with activation energies and reaction energies are presented in Fig. 2c.

In the reaction C1, the transition state 1 (TS1) is characterized by the O1-C2 bond cleavage of the epoxide and approach of O1 and C1 to the Br1 and H1 atoms of the OH group (Fig. 2a) with E_a = 30.7 kcal/mol. A gradual decrease of the distance between the atoms Br1-C2 and H1-O1 was observed from IN to intermediate 1 (IM1) (Fig. S9), suggesting the epoxide activation due to the H-bond interaction between H1-O1, and a nucleophilic attack of Br1 to C2. In TS2, the Br1 atom binds to the C2 atom of the epoxide, while the CO_2 molecule approaches the O1 atom of the epoxide (Fig. 2a and Fig. S9). The E_a of this process is equal to 3.1 kcal/mol which reflects the simplicity and rapidness of the step. In TS3, the O3 atom approaches the C2 atom of the SC molecule and simultaneously the Br1-C2 interaction weakens by increasing distance between Br1 and C2 (Fig. 2a and Fig. S9). This means an intra-molecular displacement of the halide anion (Br1) by a nucleophilic attack of oxygen (O3) to the C2. The TS3 is characterized by E_a = 34.8 kcal/mol. Hence, TS3 is the rate determining step for this pathway while the TS2 is the easiest to overcome.

In TS1 of the reaction C2, the O1-C2 bond is cleaved similarly to C1, but with a lower E_a of 26 kcal/mol leading to Br1-C2 bond formation in IM1 (Fig. 2b and Fig. S10). Consequently, IM1 shifts to TS2 by CO_2 approaching the epoxide with E_a = 2.3 kcal/mol and Br1 atom reaching

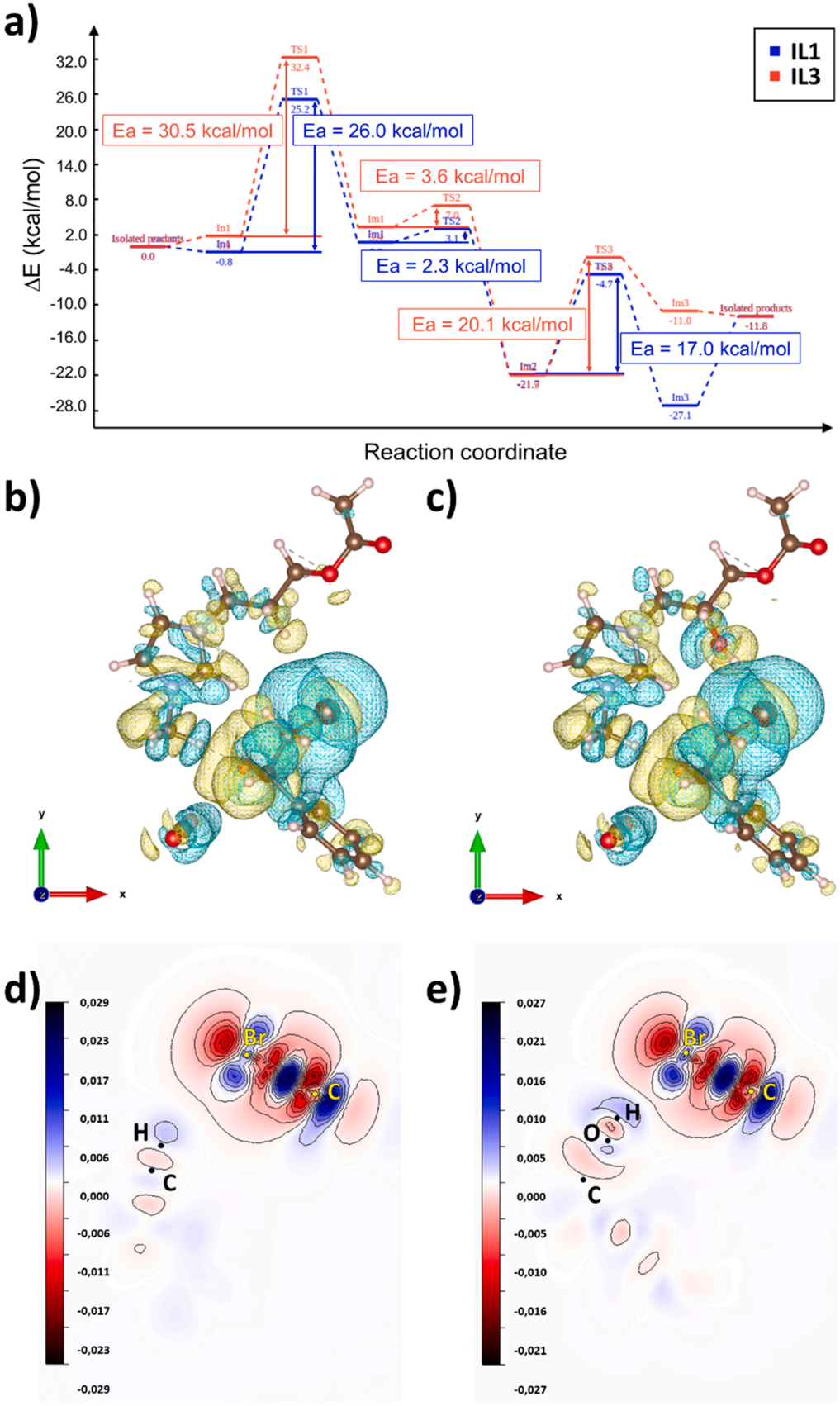

Fig. 3. a) Comparison of potential energy profiles with **IL1** and **IL3** comparison of charge density difference maps of IM1 at isovalue 0.0008 a.u. for reaction C2 with b) **IL3** and c) **IL1** and comparison of 2D slices for C2 with d) **IL3** and e) **IL1**.

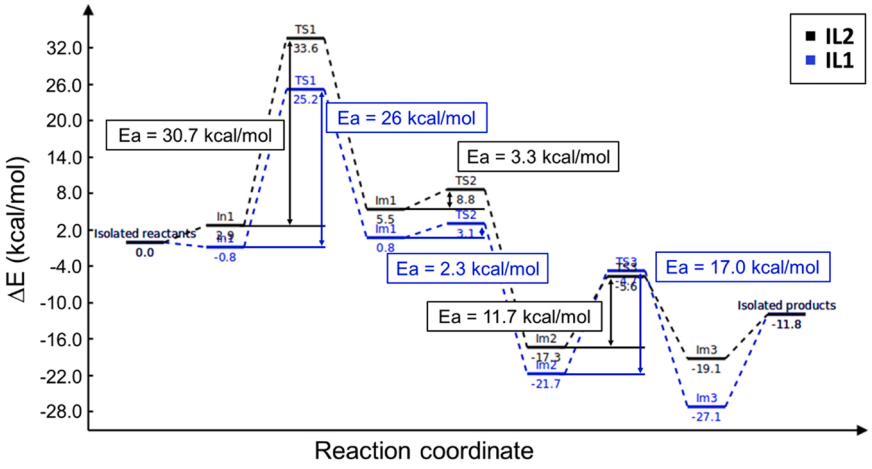

Fig. 4. Comparison of reaction coordinates of C2 with **IL1** (Br) and **IL2** (Cl).

C2 atom of epoxide. Both TSs have lower values of activation energy compared to reaction C1. Eventually, IM2 passes to the final state via the TS3, forming O2-C2 bond of the resulting SC molecule. This step is accompanied by E_a = 17 kcal/mol and compared to C1 the rate determining step is TS1.

In summary, due to lower activation energies observed, the C2 is the most plausible mechanism to occur. For this reason, the rest of the calculations were performed focusing on C2.

3.1.1. *Effect of hydroxyl group*

Having determined the reaction mechanism of the cycloaddition of CO_2 to styrene oxide employing **IL1** as catalyst, further analyses of the influence of hydroxyl group and halogen ion have been performed (**IL1** and **IL3**). The complete results of the reaction energy values in each pathway can be seen in supporting information (Table S5 and S6) and a comparison of the reaction coordinates is shown in the Figure3a.

In Fig. 3 can be observed that the presence of the hydroxyl group (**IL1**) favours the reaction by reducing the E_a of all reaction steps, including the rate determining step. Indeed, the value of E_a is higher for the system with **IL3** during all transformations to TSs (4.5 kcal/mol in TS1, 1.3 kcal/mol in TS2 and 3.1 kcal/mol in TS3). The largest difference in E_a is observed when the IN enters TS1. Therefore, the -OH group has a profound effect on all relevant catalytic steps but is mostly involved in the CO_2 cycloaddition reaction by activating epoxide molecule and opening of the epoxide ring.

The structure of IM1 with and without the presence of -OH group were visualized (Fig. 3b and c) along with the charge density difference maps and 2D slices (Fig. 3d and e) to understand the low reaction energy of IM1 from reaction C2 and its difference in comparison to the system without hydroxyl groups. A larger distance between the Br1-H1 atoms of the system with **IL3** compared to the system with **IL1**, namely 2.323 Å. Besides, the distance between the Br1-C2 atoms is smaller in a system with **IL3**, namely 2.001 Å. Therefore, the –OH group affects the Br atom to some extent and its interaction with the C2 atom of the epoxide.

3.1.2. *Influence of halogen ion*

The evaluation the anion (Br or Cl) effect was also performed by computational simulation (Fig. 4).

We can observe that the reaction coordinate of reaction C2 with **IL2** has a similar direction compared to reaction C2 with **IL1** and differs mainly in the activation energies of TS1 and TS2. The highest value of E_a is reached in TS1 with a value of 30.7 kcal/mol. At TS2 the E_a reaches 3.3 kcal/mol. In the case of TS3, the E_a of reaction C2 with **IL2** reaches lower values than the E_a of reaction C2 with **IL1**, namely 11.7 kcal/mol. Therefore, the system with **IL1** has lower values of E_a, which corresponds with the experimental results shown below. In terms of the reaction mechanism, the halide ions have the most significant effect on TS1, when the epoxide ring is being opened and the anion work as nucleophile.

3.2. *DFT calculations: cyclic oxidation of styrene*

The next objective was to conjugate the cycloaddition and the epoxidation reactions in one-pot using a single catalytic system. To this end, computational simulations were performed for the epoxidation of the styrene molecule in the presence of **IL1** and TBHP as oxidant (Figs. S3 and Tables S2-S3). Four possible reaction pathways were found (E1, E2, E3 and E4) as observed in Fig. 5a (Fig. S11, S12 and Table S7). The E_a is indicated by the reaction coordinates (Fig. 5e).

For reaction E1, E2 and E3 (Fig. 5a–c), the same initial state of epoxidation (IN_E) was determined in which the styrene molecule with the C2 atom is located near the Br1 atom of IL and at the same time near the O2 atom of TBHP.

Firstly, the system was simulated according to the proposed reaction mechanism by different studies (Fig. 1a) [47–49]. This resulted in the reaction E1 with formation of hypobromite OBr^- with $d_{(Br1\text{-}O2)}$ = 1.831 Å and H1-O1 bond formation with $d_{(H1\text{-}O1)}$ = 0.989 Å. The activation energy of this step was 31.8 kcal/mol (Fig. 5a). Furthermore, there are two possible ways of TBHP interacting with a styrene molecule. The reaction E2 is characterized by O2-C2 and O1-C3 bonds formation between atoms of TBHP and styrene (Fig. 5b). Compared to activation energy of E1, reaction E2 demands lower activation energy required to enter the TS1, 12 kcal/mol (Fig. 5e). As a result, the formation of a diol is more probable to occur by attaching the O1 and O2 atoms to the C2 and C3 atoms of styrene. In reaction E3, a similar TS1 occurs with minor differences in distances between atoms. From TS1, the system transitions to IM1 where desired styrene epoxide is formed by C3-O2 bond formation ($d_{(C3\text{-}O2)}$ = 1.467 Å). The E_a of 16 kcal/mol is required for the presented step. This implies that reaction E2 and E3 are competitive with the formation of a diol molecule predominating due to the similar values of activation energy. In the reaction E4 a different initial state (IN_{E4}) was evaluated with O2 atom oriented towards the C3 atom of styrene. During TS1 O1-O2 bond of TBHP is cleaved and subsequently in IM1 C3-O2 and Br1-C2 bonds are formed (C3 $d_{(C3\text{-}O2)}$ = 1.429 Å and $d_{(Br1\text{-}C2)}$ = 1.999 Å). The system passes to TS2, where the H1 is separated from O2 and attached to O1 atom of TBHP residue ($d_{(H1\text{-}O1)}$ = 1.896 Å). Regarding the activation energy, reaction E4 is least likely to occur because the E_a value for conversion to TS1 is incomparably higher than for reaction E1, E2 and E3, namely 66.8 kcal/mol. The results show that the formation of hypobromite is overshadowed by formation of diol and we can assume that reaction E2 will decrease the yield of essential styrene oxide.

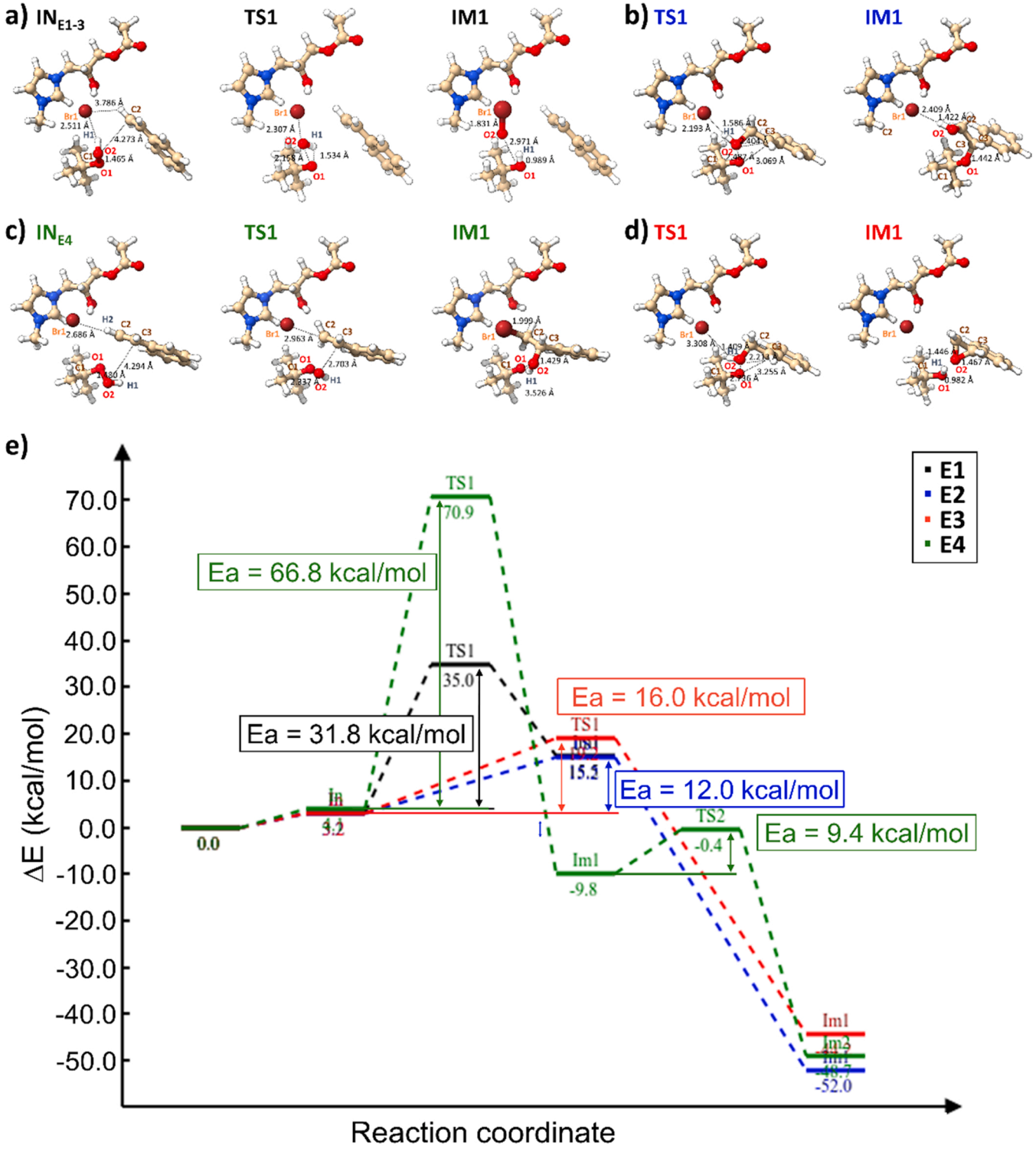

Fig. 5. Optimised initial states, TSs, and final states of a) E1, b) E2, c) E4 and d) E3, e) comparison of reaction coordinates of E1, E2, E3 and E4.

4. Experimental results

To validate the results of DFT calculations similar to those modelled were synthesized and studied as catalysts for the oxidative carboxylation of olefins. In order to focus on the hydroxyl group, and since the ester group of the IL do not present any effect on the catalysis, the ILs used as model for the experimental part were prepared without this moiety (**IL1.1** = 1-(2-hydroxypropyl)-imidazolium bromide, **IL2.1** = 1-(2-hydroxypropyl)-imidazolium chloride). Similar to the DFT calculation, the epoxidation and cycloaddition reaction were firstly evaluated independently (Table 1, entries 1–9), followed by sequential (Table 1, entries 10–13) and as one-pot reactions (Table 1, entries 14–15) and the results have been compared to the literature [5]. .

For the epoxidation reaction, IL containing Br (**IL1.1**) and Cl (**IL2.1**) were tested as catalyst. The Cl demonstrate higher selectivity (89 %) to produce styrene oxide (SO) (Table 1, entry 2). When Br was employed as the anion of the IL, the production of diol is favoured, similar to observed in the DFT calculation (Table 1, entry 2). In the absence of

Table 1
Evaluation of ILs as catalyst CO_2 valorisation to produce cyclic carbonate from epoxide and alkenes.

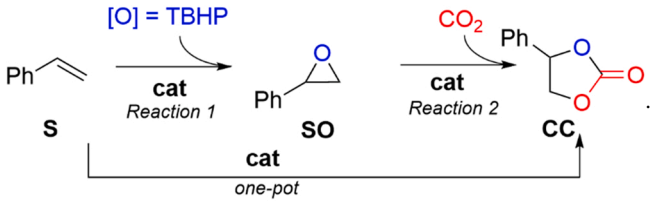

Entry	Catalyst[a]	Reaction	Temp. (°C)	P (bar)	Time (h)	Conv. S (%)[b]	Conv. SO (%)[c]	Sel. (SO). (%)[d]	Sel. (CC). (%)[e]
1	IL1.1(Br)	1	100	-	2	55	-	0[e]	-
2	IL2.1 (Cl)	1	100	-	2	66	-	89	-
3	-	1	100	-	2	4	-	3	-
4	IL2.1(Cl)	2	150	5	4	-	>99	-	76
5	BMI.Cl[5]	2	150	5	4	-	>99	-	46
6	BMI.Br[5]	2	150	5	4	-	>99	-	>99
7	IL2.1(Cl)	2	100	5	4	-	>99	-	80
8	BMI.Br[5]	2	100	5	4	-	70	-	>99
9	SIL (Cl)	2	100	5	4	-	>99	-	>99
10	IL2.1(Cl)	1;2	100;100	5	2;4	95	-	-	28
11	IL1.1(Br)	1;2	100;100	5	2;4	-	-	-	0[f]
12	SIL(Cl)	1;2	100;100	5	2;4	52	-	-	0[g]
13	BMI.Br[5]	1;2	100;150	4	2;24	>99	-	-	63
14	IL2.1(Cl)	One-pot	100	5	6	56	-	-	11
15	BMI.Br[5]	One-pot	100	4	6	74	-	-	15

Reaction condition: substrate (5 mmol), catalyst (0.5 mmol), CO_2 (5 bar), TBHP (7.5 mmol). See methodology for each reaction in experimental section. [a]IL1.1 = 1-(2-hydroxypropyl)-imidazolium bromide, IL2.1 = 1-(2-hydroxypropyl)-imidazolium chloride, BMI.Cl = 1-butyl-3-methylimidazolium chloride, BMI.Br = 1-butyl-3-methylimidazolium bromide. [b] Conversion of styrene (S) calculated by ^{1}H NMR. [c]Conversion of styrene oxide (SO) calculated by ^{1}H NMR. [d] Selectivity to form SO calculated by ^{1}H NMR. [e]Global selectivity to cyclic carbonate (CC) calculated by ^{1}H NMR. [f] diol as major byproduct. [g] Aldehyde and diol as major byproducts.

catalyst only 4 % of conversion was observed (Table 1, entry 3).

In the cycloaddition reaction, we can observe that the presence of hydroxyl group (**IL2.1**) increase the selectivity compared to alkyl chain non-functionalized (BMI.Cl) (entries 4–5). Compared to our previous work, it was possible to increase the activity of catalyst even when reducing the temperature from 150 °C to 100 °C (entries 4–7). Higher conversion (>99 %) was observed for the **IL2.1** at 100 °C compared with BMI.Br (70 %) [5]. However, the selectivity for chloride anion still smaller than bromide, due to the hygroscopicity of the catalyst. The higher activity of Br ion was also observed with DFT calculations in form of activation energy and reaction energy. This can be attributed to the higher nucleophilic character of Br [5]. Such properties allow further ring opening of the epoxide that according to DFT calculation is the determining step of reaction (TS). To reduce the hydrophilicity and create a bifunctional catalyst that can be active for both reactions (epoxidation and cycloaddition) a supported ionic liquid (**SIL**) material with the same IL moiety and Cl as anion was tested (entry 9). Same **SIL** have been previously used to prepare 3D printed catalytic columns for the CO_2 cycloaddition to epoxide [33]. The cyclic carbonate was obtained with fully conversion and selectivity. In this case, the presence of the hydroxyl group combined with less hydrophilicity of **SIL** compensate the lower nucleophilicity of Cl. This resulted in a similar selectivity when Br and Cl anion were employed (Table 1, entries 8 and 9, respectively).

Further the combination of reactions was tested. Firstly, the sequential reaction was evaluated (Table 1, entries 7–9). Despite the **IL2.1** and **SIL** present best activity to catalyse the cycloaddition reaction than BMI.Br, the opposite was observed for the combination of reaction 1 and 2. Less conversion (76–95 %) and selectivity (28–50 %) was observed compared to the previous work using BMI.Br (conversion > 99 %, selectivity 63 %) (Table 1, entries 10–13). One-pot synthesis was also evaluated, however less conversion and selectivity were obtained compared to the sequential reaction (Table 1, entries 14–15) producing diol as by-product. These results reinforce the DFT calculations, where the diol formation is less energetic, with E_a around 12–16 kcal/mol, meanwhile the epoxide formation presented 66.8 kcal/mol using similar ImILs catalyst.

5. Conclusions

The reaction mechanism of CO_2 cycloaddition using multifunctional Ils containing hydroxyl groups close to the imidazolium ring were evaluated using DFT simulations. Two reaction pathways were observed, both with the determining step observed in TS1, characterized by the epoxide ring opens. The results showed that reaction C2 has the lowest E_a at TS1, namely 26.0 kcal/mol. The effect of the cation and anion change were studied, and both present important role in the TS1. The cation activates the epoxide by H-bond, meanwhile the anion works a nucleophile. The cation containing hydroxyl group showed lowers the activation energy compared to the non-substituted cation. The effects observed were consistent with the choice of halide as anion, with lower values of activation energies were observed for bromide, since it is a stronger nucleophile compared to the chloride. Comparing with the experimental results, it was possible to establish that the presence of hydroxyl group in the cation structure can compensate the poorest nucleophilicity of chloride, and similar results between both anions were observed.

The viability of using immobilisable ILs as bifunctional catalyst for one-pot or sequential oxidative carboxylation of olefins with CO_2 was evaluated by DFT simulations. The styrene oxidation to styrene oxide showed that the reaction using simulated IL can take place via 4 reaction pathways with most likely occurring the formation of a diol as a competitive reaction with an E_a of 12 kcal/mol. The obtained values show that the one-step synthesis cyclic carbonate is not favored using similar IL-based materials. This suggests that the use of sequential reactions employing different catalysts or the spatial confinement in heterogeneous supports can be smart alternatives to overcome this problem.

The experimental results validated the DFT calculations. The ILs demonstrate great activity and selectivity in the CO_2 cycloaddition reaction. However, when combined with the epoxidation, there is a competition between the formation of diol and epoxide with a more

favourable the formation of diol. In addition, it was possible to observe that the chloride-based catalysts demonstrate better selectivity compared to Br catalyst for the one-pot reaction. Despite the Br^- being highly activity to the cycloaddition, it was found to be not selective for the epoxidation reaction.

CRediT authorship contribution statement

M.Z., N.P. and V.S. designed the experiments. M.Z. performed the experimental part. N.P performed the DFT calculation. M.Z., V.S. E.G.V. validate the results. M.Z. and V.S. conceived the project, were the responsible for funding acquisition. M.Z. and N.P wrote the original draft. All the authors contributed to the discussions, review and editing.

Declaration of Competing Interest

The authors declare that they have no known competing financial interests or personal relationships that could have appeared to influence the work reported in this paper.

Data availability

Data will be made available on request.

Acknowledgments

This work has been supported by Universitat Jaume I (UJI-B2019-40 and UJI-B2020-44) and RTI2018-098233-B-C22 y C21 (FEDER/ /Ministerio de Ciencia e Innovación – Agencia Estatal de Investigación). MZ and VS thank the funding received from the European Union's Horizon 2020, European Union research and innovation programme under the Marie Skłodowska-Curie Individual Fellowships (GA no. 101026335). VS thanks Generalitat Valenciana (CIDEGENT 2018/036) for funding. NP thanks for the support by the Scientific Grant Agency of the Ministry of Education, Science, Research, and Sport of the Slovak Republic project no. VEGA 1/0095/21 and Connecting Europe Facility of the European Union for Erasmus + funding. The authors are grateful to the SCIC of the Universitat Jaume I for technical support.

Appendix A. Supporting information

Supplementary data associated with this article can be found in the online version at doi:10.1016/j.cattod.2023.114128.

References

[1] S. Roy, S.C. Peter, Thermochemical CO2 Reduction, Advances in the Chemistry and Physics of Materials, pp. 399–428.
[2] C. Liang, Y. Chen, M. Wu, K. Wang, W. Zhang, Y. Gan, H. Huang, J. Chen, Y. Xia, J. Zhang, S. Zheng, H. Pan, Green synthesis of graphite from CO_2 without graphitization process of amorphous carbon, Nat. Commun. 12 (2021) 119.
[3] IPCC, 2022: Climate Change 2022: Impacts, Adaptation, and Vulnerability, in: D.C. R.H.-O. Pörtner, M. Tignor, E.S. Poloczanska, K. Mintenbeck, A. Alegría, M. Craig, S. Langsdorf, S. Löschke, V. Möller, A. Okem, B. Rama (Eds.), Contribution of Working Group II to the Sixth Assessment Report of the Intergovernmental Panel on Climate Change Cambridge University Press. In Press, 2022, IPCC, 2022.
[4] C. Maeda, Y. Miyazaki, T. Ema, Recent progress in catalytic conversions of carbon dioxide, Catal. Sci. Technol. 4 (2014) 1482–1497.
[5] A.-L. Girard, N. Simon, M. Zanatta, S. Marmitt, P. Gonçalves, J. Dupont, Insights on recyclable catalytic system composed of task-specific ionic liquids for the chemical fixation of carbon dioxide, Green. Chem. 16 (2014) 2815–2825.
[6] L. Guo, K.J. Lamb, M. North, Recent developments in organocatalysed transformations of epoxides and carbon dioxide into cyclic carbonates, Green. Chem. 23 (2021) 77–118.
[7] A. Saravanan, P. Senthil kumar, D.-V.N. Vo, S. Jeevanantham, V. Bhuvaneswari, V. Anantha Narayanan, P.R. Yaashikaa, S. Swetha, B. Reshma, A comprehensive review on different approaches for CO_2 utilization and conversion pathways, Chem. Eng. Sci. 236 (2021), 116515.
[8] S. Saeidi, S. Najari, V. Hessel, K. Wilson, F.J. Keil, P. Concepción, S.L. Suib, A. E. Rodrigues, Recent advances in CO_2 hydrogenation to value-added products — Current challenges and future directions, Prog. Energy Combust. Sci. 85 (2021), 100905.
[9] C.-C. Su, M. He, R. Amine, Z. Chen, R. Sahore, N. Dietz Rago, K. Amine, Cyclic carbonate for highly stable cycling of high voltage lithium metal batteries, Energy Storage Mater. 17 (2019) 284–292.
[10] F. Ouhib, L. Meabe, A. Mahmoud, B. Grignard, J.-M. Thomassin, F. Boschini, H. Zhu, M. Forsyth, D. Mecerreyes, C. Detrembleur, Influence of the cyclic versus linear carbonate segments in the properties and performance of CO_2-sourced polymer electrolytes for lithium batteries, ACS Appl. Polym. Mater. 2 (2020) 922–931.
[11] A. Jordan, C.G.J. Hall, L.R. Thorp, H.F. Sneddon, Replacement of less-preferred dipolar aprotic and ethereal solvents in synthetic organic chemistry with more sustainable alternatives, Chem. Rev. 122 (2022) 6749–6794.
[12] B. Schäffner, F. Schäffner, S.P. Verevkin, A. Börner, Organic carbonates as solvents in synthesis and catalysis, Chem. Rev. 110 (2010) 4554–4581.
[13] H.L. Parker, J. Sherwood, A.J. Hunt, J.H. Clark, Cyclic carbonates as green alternative solvents for the heck reaction, ACS Sustain. Chem. Eng. 2 (2014) 1739–1742.
[14] Z. Abdel Baki, H. Dib, T. Sahin, Overview: polycarbonates via ring-opening polymerization, differences between six- and five-membered cyclic carbonates: inspiration for green alternatives, Polymers 14 (2022) 2031.
[15] F. Suriano, O. Coulembier, J.L. Hedrick, P. Dubois, Functionalized cyclic carbonates: from synthesis and metal-free catalyzed ring-opening polymerization to applications, Polym. Chem. 2 (2011) 528–533.
[16] D.C. Webster, Cyclic carbonate functional polymers and their applications, Prog. Org. Coat. 47 (2003) 77–86.
[17] H. Büttner, L. Longwitz, J. Steinbauer, C. Wulf, T. Werner, Recent developments in the synthesis of cyclic carbonates from epoxides and CO_2, Top. Curr. Chem. 375 (2017) 50.
[18] A. Monfared, R. Mohammadi, A. Hosseinian, S. Sarhandi, P.D. Kheirollahi Nezhad, Cycloaddition of atmospheric CO_2 to epoxides under solvent-free conditions: a straightforward route to carbonates by green chemistry metrics, RSC Adv. 9 (2019) 3884–3899.
[19] A.J. Kamphuis, F. Picchioni, P.P. Pescarmona, CO_2-fixation into cyclic and polymeric carbonates: principles and applications, Green. Chem. 21 (2019) 406–448.
[20] J. Zhu, J. Liu, Y. Machain, B. Bonnett, S. Lin, M. Cai, M.C. Kessinger, P.M. Usov, W. Xu, S.D. Senanayake, D. Troya, A.R. Esker, A.J. Morris, Insights into CO_2 adsorption and chemical fixation properties of VPI-100 metal–organic frameworks, J. Mater. Chem. A 6 (2018) 22195–22203.
[21] Z.-J. Li, J.-F. Sun, Q.-Q. Xu, J.-Z. Yin, Homogeneous and heterogeneous ionic liquid system: promising "ideal catalysts" for the fixation of CO_2 into cyclic carbonates, ChemCatChem 13 (2021) 1848–1866.
[22] X.-D. Lang, L.-N. He, Green catalytic process for cyclic carbonate synthesis from carbon dioxide under mild conditions, Chem. Rec. 16 (2016) 1337–1352.
[23] O. Martínez-Ferraté, G. Chacón, F. Bernardi, T. Grehl, P. Brüner, J. Dupont, Cycloaddition of carbon dioxide to epoxides catalysed by supported ionic liquids, Catal. Sci. Technol. 8 (2018) 3081–3089.
[24] K. Kiatkittipong, M.A.A. Mohamad Shukri, W. Kiatkittipong, J.W. Lim, P.L. Show, M.K. Lam, S. Assabumrungrat, Green pathway in utilizing CO_2 via cycloaddition reaction with epoxide—a mini review, Processes 8 (2020) 548.
[25] M. He, Y. Sun, B. Han, Green carbon science: scientific basis for integrating carbon resource processing, utilization, and recycling, Angew. Chem. Int. Ed. 52 (2013) 9620–9633.
[26] Y. Wang, L. Guo, L. Yin, Progress in the heterogeneous catalytic cyclization of CO_2 with epoxides using immobilized ionic liquids, Catal. Lett. 149 (2019) 985–997.
[27] J.N. Appaturi, R.J. Ramalingam, M.K. Gnanamani, G. Periyasami, P. Arunachalam, R. Adnan, F. Adam, M.D. Wasmiah, H.A. Al-Lohedan, Review on carbon dioxide utilization for cycloaddition of epoxides by ionic liquid-modified hybrid catalysts: effect of influential parameters and mechanisms insight, Catalysts 11 (2021) 4.
[28] R.L. Vekariya, A review of ionic liquids: applications towards catalytic organic transformations, J. Mol. Liq. 227 (2017) 44–60.
[29] D.-W. Kim, R. Roshan, J. Tharun, A. Cherian, D.-W. Park, Catalytic applications of immobilized ionic liquids for synthesis of cyclic carbonates from carbon dioxide and epoxides, Korean J. Chem. Eng. 30 (2013) 1973–1984.
[30] N. Subasree, J.A. Selvi, Imidazolium based ionic liquid derivatives; synthesis and evaluation of inhibitory effect on mild steel corrosion in hydrochloric acid solution, Heliyon 6 (2020), e03498.
[31] S. Lian, C. Song, Q. Liu, E. Duan, H. Ren, Y. Kitamura, Recent advances in ionic liquids-based hybrid processes for CO_2 capture and utilization, J. Environ. Sci. 99 (2021) 281–295.
[32] V.B. Saptal, B.M. Bhanage, Bifunctional ionic liquids derived from biorenewable sources as sustainable catalysts for fixation of carbon dioxide, ChemSusChem 10 (2017) 1145–1151.
[33] D. Valverde, R. Porcar, M. Zanatta, S. Alcalde, B. Altava, V. Sans, E. García-Verdugo, Towards highly efficient continuous-flow catalytic carbon dioxide cycloadditions with additively manufactured reactors, Green. Chem. 24 (2022) 3300–3308.
[34] J. Sun, S.-i Fujita, B.M. Bhanage, M. Arai, One-pot synthesis of styrene carbonate from styrene in tetrabutylammonium bromide, Catal. Today 93–95 (2004) 383–388.
[35] K. Jasiak, T. Krawczyk, M. Pawlyta, A. Jakóbik-Kolon, S. Baj, One-pot synthesis of styrene carbonate from styrene and CO_2 over the nanogold-ionic liquid catalyst, Catal. Lett. 146 (2016) 893–901.
[36] J. Liu, G. Yang, Y. Liu, D. Wu, X. Hu, Z. Zhang, Metal-free imidazolium hydrogen carbonate ionic liquids as bifunctional catalysts for the one-pot synthesis of cyclic carbonates from olefins and CO_2, Green. Chem. 21 (2019) 3834–3838.

[37] M. Cui, F. Shamsa, Ionic liquid supported on DFNS nanoparticles catalyst in synthesis of cyclic carbonates by oxidative carboxylation, Catal. Lett. 152 (2022) 87–97.
[38] G. Long, K. Su, H. Dong, T. Zhao, C. Yang, F. Liu, X. Hu, Straightforward construction of amino-functionalized ILs@SBA-15 catalysts via mechanochemical grafting for one-pot synthesis of cyclic carbonates from aromatic olefins and CO_2, J. CO_2 Util. 59 (2022), 101962.
[39] J.P. Perdew, K. Burke, M. Ernzerhof, Generalized gradient approximation made simple, Phys. Rev. Lett. 77 (1996) 3865–3868.
[40] M. Ernzerhof, G.E. Scuseria, Assessment of the Perdew-Burke-Ernzerhof exchange-correlation functional, J. Chem. Phys. 110 (1999) 5029.
[41] P. Giannozzi, S. Baroni, N. Bonini, M. Calandra, R. Car, C. Cavazzoni, D. Ceresoli, G.L. Chiarotti, M. Cococcioni, I. Dabo, A. Dal Corso, S. Fabris, G. Fratesi, S. de Gironcoli, R. Gebauer, U. Gerstmann, Ch Gougoussis, A. Kokalj, M. Lazzeri, L. Martin-Samos, N. Marzari, F. Mauri, R. Mazzarello, S. Paolini, A. Pasquarello, L. Paulatto, C. Sbraccia, S. Scandolo, G. Sclauzero, A.P. Seitsonen, A. Smogunov, P. Umari, R.M. Wentzcovitch, QUANTUM ESPRESSO: a modular and open-source software project for quantum simulations of materials, J. Phys.: Condens. Matter 21 (2009), 395502.
[42] P. Giannozzi, O. Andreussi, T. Brumme, O. Bunau, M.B. Nardelli, M. Calandra, R. Car, C. Cavazzoni, D. Ceresoli, M. Cococcioni, N. Colonna, I. Carnimeo, A. Dal Corso, S. de Gironcoli, P. Delugas, R.A. DiStasio Jr, A. Ferretti, A. Floris, G. Fratesi, G. Fugallo, R. Gebauer, U. Gerstmann, F. Giustino, T. Gorni, J. Jia, M. Kawamura, H.-Y. Ko, A. Kokalj, E. Küçükbenli, M. Lazzeri, M. Marsili, N. Marzari, F. Mauri, N. L. Nguyen, H.-V. Nguyen, A. Otero-de-la-Roza, L. Paulatto, S. Poncé, D. Rocca, R. Sabatini, B. Santra, M. Schlipf, A.P. Seitsonen, A. Smogunov, I. Timrov, T. Thonhauser, P. Umari, N. Vast, X. Wu, S. Baroni, Advanced capabilities for materials modelling with QUANTUM ESPRESSO, J. Od. Phys.: Condens. Matter 29 (2017), 465901.
[43] P.E. Blöchl, Projector augmented-wave method, Phys. Rev. B 50 (1994) 17953–17979.
[44] G. Henkelman, B.P. Uberuaga, H. Jónsson, A climbing image nudged elastic band method for finding saddle points and minimum energy paths, J. Chem. Phys. 113 (2000) 9901.
[45] G. Henkelman, H. Jónsson, Improved tangent estimate in the nudged elastic band method for finding minimum energy paths and saddle points, J. Chem. Phys. 113 (2000) 9978.
[46] R.A. Angnes, ricalmang/mechaSVG v.0.0.8, Zenodo 2020, 2020.
[47] J.W. Comerford, I.D.V. Ingram, M. North, X. Wu, Sustainable metal-based catalysts for the synthesis of cyclic carbonates containing five-membered rings, Green. Chem. 17 (2015) 1966–1987.
[48] A. Rehman, V.C. Eze, M.F.M.G. Resul, A. Harvey, Kinetics and mechanistic investigation of epoxide/CO_2 cycloaddition by a synergistic catalytic effect of pyrrolidinopyridinium iodide and zinc halides, J. Energy Chem. 37 (2019) 35–42.
[49] M. Cokoja, M.E. Wilhelm, M.H. Anthofer, W.A. Herrmann, F.E. Kühn, Synthesis of cyclic carbonates from epoxides and carbon dioxide by using organocatalysts, ChemSusChem 8 (2015) 2436–2454.
[50] J. Sun, S.-i Fujita, B.M. Bhanage, M. Arai, Direct oxidative carboxylation of styrene to styrene carbonate in the presence of ionic liquids, Catal. Commun. 5 (2004) 83–87.